Pattern Recognition and Artificial Intelligence
E.S. Gelsema and L.N. Kanal (Editors)

PATTERN RECOGNITION BY DETECTION OF LOCAL SYMMETRIES

Josef BIGÜN

Computer Vision Laboratory
Linköping University
Department of Electrical Engineering
S-581 83 Linköping Sweden

The symmetries in a neighbourhood of a gray value image are modelled by conjugate harmonic function pairs. These are shown to be a suitable curve linear coordinate pair, in which the model represents a neighbourhood. In this representation the image parts, which are symmetric with respect to the chosen function pair, have iso-gray value curves which are simple lines or parallel line patterns. The detection is modelled in the special Fourier domain corresponding to the new variables by minimizing an error function. It is shown that the minimization process or detection of these patterns can be carried out for the whole image entirely in the spatial domain by convolutions. What will be defined as the partial derivative image is the image which takes part in the convolution. The convolution kernel is complex valued, as are the partial derivative image and the result. The magnitudes of the result are shown to correspond to a well defined certainty measure, while the orientation is the least square estimate of an orientation in the Fourier transform corresponding to the harmonic coordinates. Applications to four symmetries are given. These are circular, linear, hyperbolic and parabolic symmetries. Experimental results are presented.

1 INTRODUCTION

Describing events in neighbourhoods of a gray value image is an increasing need in Computer Vision. The most extensively studied event is the existence of lines and edges. Also circular patterns have been subject to investigation [9], [5], [4], [3]. The generalized Hough transform, [6], is general and accurate enough to find arbitrary curves with the drawback of being computationally demanding. In the following we will give a method for detection of a large class of symmetries in a gray value neighbourhood which is a generalization of the work done in [3], [4] for circular symmetry.

By a neighbourhood of a point will be understood the image multiplied by a window function placed at the point. For its behaviour to be satisfactory in practical situations we will assume this window function to be a gaussian with a sufficiently large standard deviation instead of a sharp window. But the method is not restricted to this choice. In Section 2, a definition of symmetry will be given by means of a pair of conjugate harmonic functions in which the neighbourhood coordinates are represented. After this representation, the neighbourhoods with iso-gray value curves associated with a linear combination of these chosen coordinates constitute the family of neighbourhoods for which the detection is developed.

The detection is based on minimization of an error function in the Fourier domain, but computed entirely in the spatial domain. In Section 3, this minimization process is shown to be a convolution of the complex valued partial derivative image with a complex valued filter. The result delivers an angle corresponding to a subclass of neighbourhoods within

the family of the neighbourhoods the a priori chosen function pair can handle. By changing this angle, all patterns in the symmetry model can be reached which is in analogy of a class of lines and edges with the same orientation. All lines and edges are covered by changing the orientation of the latter class. In fact, in Section 4 it is shown that lines and edges can be modelled in this general framework just as any other symmetry.

Besides the orientation of the found symmetry, the minimization process delivers a certainty defined by the minimum and maximum error. The higher the significance of the found symmetry orientation for the neighbourhood, the higher this certainty becomes. Also a non-energy dependent certainty measure is derived, which is useful for pictures with different light conditions in different parts of the picture. In Section 4 applications and experimental results are given.

Four symmetry models are covered by using the general methodology given in Sections 3 and 4. These are circular, linear, hyperbolic and parabolic symmetries. The conjugate harmonic function pairs are easily established by observing that all analytic functions' real and imaginary parts are such pairs. The analytic functions connected with the symmetries mentioned are the elementary functions: $\log z$, z, z^2 and $\sqrt{z}$.

2 MODELING THE LOCAL NEIGHBOURHOODS BY HARMONIC FUNCTIONS

Let $u(x,y)$ be a *harmonic function* defined in the neighbourhood, that is, it is continuous together with its partial derivatives of the first two orders and satisfies the *Laplace's equation:*

$$\Delta u = \frac{\partial^2 u}{\partial x^2} + \frac{\partial^2 u}{\partial y^2} = 0. \tag{1}$$

Due to the linear character of Laplace's equation, the linear combinations of the harmonic functions are also harmonic. If two harmonic functions u and v satisfy the *Cauchy-Riemann equations:*

$$\frac{\partial u}{\partial x} = \frac{\partial v}{\partial y}, \quad \frac{\partial u}{\partial y} = -\frac{\partial v}{\partial x} \tag{2}$$

then v is said to be the *conjugate harmonic function* of u. The imaginary part of any analytic function is the conjugate harmonic function of the real part. In general v does not need to be a single valued function even if u is. Here we will assume both u and v to be single valued. By definition, (2), a curve pair defined by:

$$\xi = u(x,y) \tag{3}$$
$$\eta = v(x,y) \tag{4}$$

are orthogonal to each other at their intersection points for any constants ξ and η. For non trivial $u(x,y)$ and $v(x,y)$, (3-4) define a coordinate transformation which is reversible almost everywhere.

Consider a neighbourhood around a point in a gray value image. Let this neighbourhood be represented by the real function $f_1(x,y)$ which attains positive real values. For simplicity we will assume that the origin of the Cartesian coordinate system in which the neighbourhood is represented as being the considered point. Let $\bar{r} = (\xi,\eta)^t$ be defined through (3–4). The representation of the neighbourhood is then possible in these coordinates and yields $f_1(x,y) = f_2(\xi,\eta)$.

Definition 1 *The local neighbourhood $f(x,y)$ represented in its local Cartesian coordinates, is said to be symmetric with respect to the coordinates $(\xi,\eta)^t$ if there exists a one dimensional function g so that $f(x,y) = g(a\xi + b\eta)$ for some real constants, a and b. Here $(\xi,\eta)^t = (u(x,y), v(x,y))^t$ and v is the harmonic conjugate function of u.*

This definition suggests that the iso-gray value curves of a neighbourhood, which is symmetric with respect to a coordinate pair $(\xi,\eta)^t$, are *parallel lines* in this coordinate system. In the following we will develop a method to select all neighbourhoods of an image, which are symmetric with respect to an a priori chosen local coordinate transformation given by the harmonic pair $(\xi,\eta)^t = (u(x,y),v(x,y))^t$. It may be thought that every neighbourhood is first represented in its local Cartesian coordinates and then represented in the transformed coordinate system which in turn tested whether its iso-gray value curves are parallel lines. Of course we will not suggest doing all these time-consuming transformations in practice but rather their equivalents which are computationally easy to evaluate. In general a neighbourhood is not symmetric with respect to an a priori coordinate transformation. But when it is symmetric, we will observe that the energy of the neighbourhood is concentrated to a line through the origin in its Fourier transform domain corresponding to the new coordinates. Our approach will be to check whether there exists a line concentration in the local Fourier domain obtained by means of the new coordinates. But before doing this, we should specify what we mean by this special Fourier transformation and a line concentration in it.

Let the local image be represented by $f(\xi,\eta)$, then the corresponding Fourier transformation is defined as:

$$F(\omega,\varsigma) = \int_{-\infty}^{\infty}\int_{-\infty}^{\infty} \exp[-i(\omega\xi+\varsigma\eta)]f(\xi,\eta)d\xi d\eta \tag{5}$$

Here we assumed that ξ and η have the range $[-\infty,\infty]$. For cases where either of the variables have a finite range, f is put to zero outside its value set. Then the corresponding transform variable (ω or ς) constitutes a numerable periodic discrete set (Fourier series expansion in that variable). In the following, all integrations in the spatial domain should be interpreted in this sense. The inverse transform is obtained through:

$$f(\xi,\eta) = (2\pi)^{-2}\int_{-\infty}^{\infty}\int_{-\infty}^{\infty} \exp[i(\omega\xi+\varsigma\eta)]F(\omega,\varsigma)d\omega d\varsigma. \tag{6}$$

where one of the integrations is changed to a summation over a discrete periodic set if ξ or η has finite range. In the following, all integrations in the Fourier domain should be interpreted in this sense.

Theorem 1 *A symmetric neighbourhood with respect to the coordinates $(\xi,\eta)^t$, that is $f(a\xi+b\eta)$, has a Fourier transform, in these coordinates, which is concentrated to a line through the origin:*

$$(\mathcal{F}f)(\omega,\varsigma) = \frac{1}{2\pi}\delta(b\omega-a\varsigma)\int_{-\infty}^{\infty} f(t)exp(-it(a\omega+b\varsigma))dt \tag{7}$$

where δ is the dirac distribution, and the symmetry direction vector, $(a,b)^t$, has the modulus of unity:

$$\sqrt{a^2+b^2} = 1. \tag{8}$$

The proof of the theorem is straight forward and will be omitted here, [1]. As already mentioned, the initial position for determining the symmetry is the corresponding Fourier domain. Any neighbourhood in the image will then have a Fourier transform which is not necessarily concentrated to a line through the origin. We will fit the best line to the corresponding Fourier domain in the least square sense. If there exists a symmetry according to an a priori model then the error will be low. The greater the size of the minimum error, the more degradation from this symmetry will be observed. To any neighbourhood, a line through the origin of its Fourier transform, or rather its orientation, will be given together with the minimum error expressing the significance of the found symmetry. The degradation of $F(\omega,\varsigma)$ from a line $t\bar{k}_\theta = t\cdot(\cos\theta,\sin\theta)^t$ with $t\in R$, or the error in the least square estimation, will be given by:

$$E(\theta) = \int_{-\infty}^{\infty}\int_{-\infty}^{\infty} d^2(\bar{k},\bar{k}_\theta)\left|F(\bar{k})\right|^2 d\omega d\varsigma. \tag{9}$$

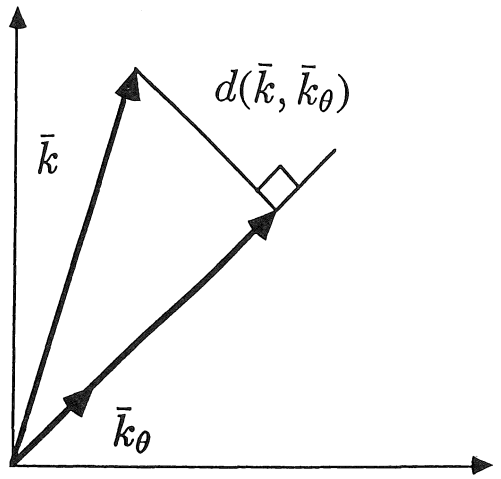

Figure 1: The figure illustrates the Euclidean distance in the special Fourier domain, $d(\bar{k}, \bar{k}_\theta)$, between the coordinate point $\bar{k}$ and the axis denoted by $\bar{k}_\theta$.

Here $d^2(\bar{k}, \bar{k}_\theta)$ is the squared Euclidean distance between the vector $\bar{k} = (\omega, \varsigma)^t$ and $\bar{k}_\theta = (\cos\theta, \sin\theta)^t$, of which the former symbolizes the transposed coordinate vector in the special Fourier domain, Figure 1. Without proof, [2], we mention the following theorem.

Theorem 2 *The double angle minimizing $E(\theta)$, e.g. $2\theta_{min}$ is given by the formula:*

$$2\theta_{min} = \tan^{-1}(\omega_d^2 - \varsigma_d^2, 2p_d) \tag{10}$$

where

$$\begin{aligned} \omega_d^2 &= \int_{-\infty}^{\infty}\int_{-\infty}^{\infty} \omega^2 |F(\omega,\varsigma)|^2 \, d\omega d\varsigma \\ \varsigma_d^2 &= \int_{-\infty}^{\infty}\int_{-\infty}^{\infty} \varsigma^2 |F(\omega,\varsigma)|^2 \, d\omega d\varsigma \\ p_d &= \int_{-\infty}^{\infty}\int_{-\infty}^{\infty} \varsigma\omega |F(\omega,\varsigma)|^2 \, d\omega d\varsigma. \end{aligned}$$

The error corresponding to the line given by θ_{min} is obtained through

$$E(\theta_{min}) = \frac{1}{2}[\omega_d^2 + \varsigma_d^2 - \sqrt{(\omega_d^2 - \varsigma_d^2)^2 + 4p_d^2}]. \tag{11}$$

Moreover, the line corresponding to the angle maximizing the error $E(\theta)$, is orthogonal to the line minimizing the error. The maximum error is given by:

$$E(\theta_{max}) = \frac{1}{2}[\omega_d^2 + \varsigma_d^2 + \sqrt{(\omega_d^2 - \varsigma_d^2)^2 + 4p_d^2}]. \tag{12}$$

Since we know that the least square error line passes through the origin, it is possible to specify it by a single real variable. We will choose the label 2θ for a line given by

$t \cdot (\cos\theta, \sin\theta)^t$. Labelling a line by the angle of 2θ instead of θ is more suitable since 2θ maps θ and $\theta + \pi$ to the same angle. This is a desirable property, since we do not want to claim that we have found two different lines when we obtain two angles differing by π.

The least square error $E(\theta_{min})$ is a positive number which we really cannot interpret if it is not related to another quantity, since we should know what is a large error and what is a small one. One way to do that, is to consider the quantity:

$$C_{f1} = E(\theta_{max}) - E(\theta_{min}) = \sqrt{(\omega_d^2 - \varsigma_d^2)^2 + 4p_d^2} \tag{13}$$

which can be used as a certainty measure for the found symmetry. This is simply a quantity which measures how much better a best fitted line is compared to the worst line. It is non-negative and is large for neighbourhoods possessing the symmetry under consideration and it decreases smoothly for the neighbourhoods degrading from this type of symmetry. This definition allows us to consolidate the obtained orientation and the corresponding symmetry to a complex number z_1, [8]:

$$z_1 = \omega_d^2 - \varsigma_d^2 + i2p_d = C_{f1} \exp(i2\theta_{min}). \tag{14}$$

Another way to interpret $E(\theta_{min})$ is to use

$$C_{f2} = \frac{E(\theta_{max}) - E(\theta_{min})}{E(\theta_{max}) + E(\theta_{min})} \tag{15}$$

as a certainty measure. Unlike C_{f1}, it is not energy dependent and $C_{f2} = 1$ if and only if $E(\theta_{min}) = 0$ which is the condition for a truly symmetric neighbourhood. Moreover it varies between 0 and 1. The closer this measure is to 1 the more significant the found symmetry is. If desired, C_{f2} and $2\theta_{min}$ can be consolidated to a complex number $z_2 = C_{f2} \exp i2\theta$ as before.

If the two symmetry models specified by the local coordinate transformations

$$(\xi_1, \eta_1) = (u_1(x,y), v_1(x,y)) \quad (\xi_2, \eta_2) = (u_2(x,y), v_2(x,y)) \tag{16}$$

are given, then can we relate the two certainty measures obtained for a neighbourhood? That is can we say that one symmetry model describes the neighbourhood better than the other when the certainty for one of them is higher? Since equality occurs for $C_{f2} \leq 1$ only when we have a truly symmetric neighbourhood and the right hand side is independent of the chosen transformations describing the symmetries, the two certainties of type C_{f2} can be related to each other. The following theorem will help us to answer the question when the certainties are of C_{f1} type.

Theorem 3 (Energy Conservation) *The sum of the maximum and the minimum error is independent of the coordinate system chosen for symmetry investigation of a given neighbourhood f:*

$$E(\theta_{max}) + E(\theta_{min}) = \int_{-\infty}^{\infty}\int_{-\infty}^{\infty} (\omega^2 + \varsigma^2)\,|F(\omega,\varsigma)|^2\, d\omega d\varsigma \tag{17}$$

$$= \int_{-\infty}^{\infty}\int_{-\infty}^{\infty} (\frac{\partial f}{\partial \xi})^2 + (\frac{\partial f}{\partial \eta})^2 d\xi d\eta \tag{18}$$

$$= \int_{-\infty}^{\infty}\int_{-\infty}^{\infty} (\frac{\partial f}{\partial x})^2 + (\frac{\partial f}{\partial y})^2 dx dy. \tag{19}$$

The Fourier transform of f in the new coordinates is F as before.

Proof: The first equality is obtained by theorem 2 the second is provided by the Parseval relation. To prove the third relation we utilize the chain rule:

$$\frac{\partial f}{\partial \xi} = \frac{\partial f}{\partial x}\frac{\partial x}{\partial \xi} + \frac{\partial f}{\partial y}\frac{\partial y}{\partial \xi}$$

and then utilize the fact that the Jacobian

$$\frac{\partial(\xi,\eta)}{\partial x \partial y} \triangleq \begin{pmatrix} \frac{\partial \xi}{\partial x} & \frac{\partial \xi}{\partial y} \\ \frac{\partial \eta}{\partial x} & \frac{\partial \eta}{\partial y} \end{pmatrix}$$

is given by

$$\frac{\partial(\xi,\eta)}{\partial x \partial y} = \begin{pmatrix} \frac{\partial \xi}{\partial x} & \frac{\partial \xi}{\partial y} \\ -\frac{\partial \xi}{\partial y} & \frac{\partial \xi}{\partial x} \end{pmatrix}$$

since $\xi = u(x,y)$ and $\eta = v(x,y)$ constitute a harmonic pair fulfilling the Cauchy–Riemann equations (2), almost everywhere. Remembering the relation

$$\frac{\partial(x,y)}{\partial \xi \partial \eta} = \left(\frac{\partial(\xi,\eta)}{\partial x \partial y}\right)^{-1} = \frac{1}{(\frac{\partial \xi}{\partial x})^2 + (\frac{\partial \xi}{\partial y})^2} \begin{pmatrix} \frac{\partial \xi}{\partial x} & -\frac{\partial \xi}{\partial y} \\ \frac{\partial \xi}{\partial y} & \frac{\partial \xi}{\partial x} \end{pmatrix}$$

we obtain

$$\frac{\partial f}{\partial \xi} = \frac{1}{(\frac{\partial \xi}{\partial x})^2 + (\frac{\partial \xi}{\partial y})^2}\left(\frac{\partial f}{\partial x}\frac{\partial \xi}{\partial x} - \frac{\partial f}{\partial y}\frac{\partial \xi}{\partial y}\right).$$

Similarly

$$\frac{\partial f}{\partial \eta} = \frac{1}{(\frac{\partial \xi}{\partial x})^2 + (\frac{\partial \xi}{\partial y})^2}\left(\frac{\partial f}{\partial x}\frac{\partial \xi}{\partial y} + \frac{\partial f}{\partial y}\frac{\partial \xi}{\partial x}\right)$$

is obtained. Thus

$$(\frac{\partial f}{\partial \xi})^2 + (\frac{\partial f}{\partial \eta})^2 = \frac{1}{(\frac{\partial \xi}{\partial x})^2 + (\frac{\partial \xi}{\partial y})^2}((\frac{\partial f}{\partial x})^2 + (\frac{\partial f}{\partial y})^2)$$

together with the variable substitution according to (3) and (4) concludes the proof.

It follows from the theorem even the certainties of type C_{f1}, can be related to each other since

$$0 \leq C_{f1} \leq E(\theta_{max}) + E(\theta_{min}) \tag{20}$$

and the right hand of the inequality is independent of the choice of the transformation for description of symmetry. Equality occurs only when the neighbourhood is truly symmetric with respect to the chosen coordinates. The closer C_{f1} is to this common upper bound, the better the chosen transformation describes the underlying symmetry.

The certainties and the orientation above are evaluated in the Fourier domain corresponding to the a priori chosen coordinate transformation. By using the Parseval relation it is possible to transfer these evaluations to the spatial domain:

$$\omega_d^2 = (2\pi)^2 \int_{-\infty}^{\infty}\int_{-\infty}^{\infty} (\frac{\partial f}{\partial \xi})^2 d\xi d\eta \tag{21}$$

$$\varsigma_d^2 = (2\pi)^2 \int_{-\infty}^{\infty}\int_{-\infty}^{\infty} (\frac{\partial f}{\partial \eta})^2 d\xi d\eta \tag{22}$$

$$p_d = (2\pi)^2 \int_{-\infty}^{\infty}\int_{-\infty}^{\infty} \frac{\partial f}{\partial \eta}\frac{\partial f}{\partial \xi} d\xi d\eta. \tag{23}$$

3 DETECTION OF LOCAL SYMMETRIES

In the previous section we have presented a model by which we could test the symmetry with respect to a fixed coordinate system in the entire image. Although (21–23) presents a way to evaluate the quantities necessary for the symmetry test of a neighbourhood in the spatial domain, it is still cumbersome to evaluate these integrals for every neighbourhood. The chain rule applied to these formulas along with the Cauchy-Riemann equations, (2), establishes:

$$z_1 = \int_{-\infty}^{\infty}\int_{-\infty}^{\infty} (\frac{\partial f}{\partial x} + i\frac{\partial f}{\partial y})^2 \exp[-i2\arg(\frac{\partial \xi}{\partial x} + i\frac{\partial \xi}{\partial y})]dxdy. \tag{24}$$

By this result, z_1 the unit incorporating the certainty and the found symmetry orientation, is ready for aproximation by discrete image data. Assume that f is a bandlimited function, that is, its Fourier transform in the Cartesian coordinates is such that it vanishes outside a bounded region. Then it is possible to reconstruct f from its discrete samples. The same is true for f's partial derivatives with respect to x and y, the functions obtained by f's products and sums with other bandlimited functions, etc.

Assume that the local neighbourhood is such a bandlimited function. Then for sufficient dense discretization

$$z_1 = \sum_j (f_{xj} + if_{yj})^2 \int_{-\infty}^{\infty}\int_{-\infty}^{\infty} \mu_j(\bar{r}) \exp[-i2\arg(\frac{\partial \xi}{\partial x} + i\frac{\partial \xi}{\partial y})]dxdy \tag{25}$$

is evaluated from the samples f_{xj} and f_{yj}. The latter are the values of the functions $\frac{\partial f}{\partial x}$ and $\frac{\partial f}{\partial y}$ at the discrete image position $\bar{r}_j$. The image given by $(f_{xj} + if_{yj})^2$ will be referred to as the *partial derivative image*. The analytic function μ_j will be called the *interpixel function* since it is the function which makes it possible to evaluate values between the image pixels. It is the function obtained by inverse Fourier transforming a region function which is 1 inside of a region and 0 outside of it. The region itself is the region in which the Fourier transform of the bandlimited function $(\frac{\partial f}{\partial x} + i\frac{\partial f}{\partial y})^2$ does not vanish. Even if a gaussian is not an ideal inter pixel function in the strict sense it is proposed to utilize as μ_j to obtain reasonable filter sizes.

Consider (25), which is a convolution with a filter with the coefficients:

$$w^j = \int_{-\infty}^{\infty} \mu_j(\bar{r}) \exp[-i2\arg(\frac{\partial \xi}{\partial x} + i\frac{\partial \xi}{\partial y})]dxdy. \tag{26}$$

The filter coefficients decrease rapidly as $\|\bar{r}_j\|$ become large when μ_j is chosen as:

$$\mu_j(\bar{r}) = \exp(-\beta\|\bar{r} - \bar{r}_j\|^2) \exp(-\alpha\|\bar{r}\|^2). \tag{27}$$

Here α controls the size of the neighbourhood and β controls the low pass character of the filter. The image should be multiplied by the gaussian term containing α to define a neighbourhood, but for convenience it is incorporated to the interpixel function, resulting in the same effect.

Since $z_2 = z_1/[E(\theta_{max}) + E(\theta_{min}))]$ and the denominator is independent of the chosen coordinate system it is easy to obtain z_2 from z_1. We will not consider the derivation of the error sum in detail. We will only mention that it is a gaussian filtering of $\left|\frac{\partial f}{\partial x} + i\frac{\partial f}{\partial y}\right|^2$ and refer to [4] for further details.

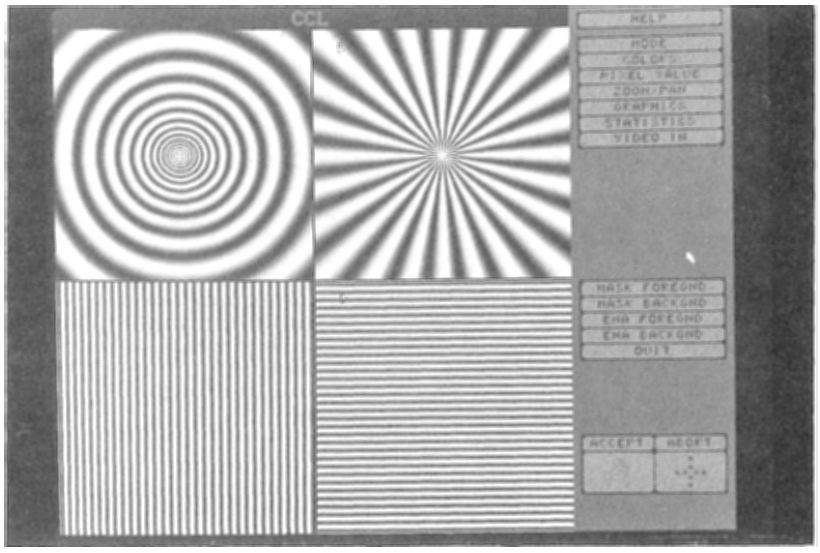

Figure 2: The figure illustrates the iso-gray value curves of a)-b) the circular symmetric harmonic function pair c)-d) linear symmetric harmonic function pair.

4 APPLICATIONS AND EXPERIMENTS

To apply the method derived above, a model for the symmetry in terms of harmonic functions and a partial derivative image,

$$(f_{xj} + if_{yj})^2 \tag{28}$$

are required. A special technique is not required to obtain f_{xj} and f_{yj}. Many methods exist in the literature for this purpose. However an efficient and easily implemented one is to convolve the image by the partial derivatives of a gaussian even though this has some drawbacks. In the experiments we have made this choice to obtain the partial derivative image.

For test purposes we define a one dimensional function g as

$$g(x) = (1 + \cos x)/2 \tag{29}$$

which is positive. The parameter x of this one dimensional function is replaced by $a\xi + b\eta$ to illustrate the different symmetries given below.

1. The function $\log z$, except for the origin, is analytic and single valued if one defines the *principal branch* as the value set. Since the imaginary part of an analytic function is the conjugate harmonic function of its real part, then

$$\log z = \ln r + i\varphi \tag{30}$$

where $r = |z|$, $\varphi = \arg(z)$ and z is the complex variable $x + iy$. Thus

$$\begin{aligned} \xi &= \ln r \\ \eta &= \varphi \end{aligned}$$

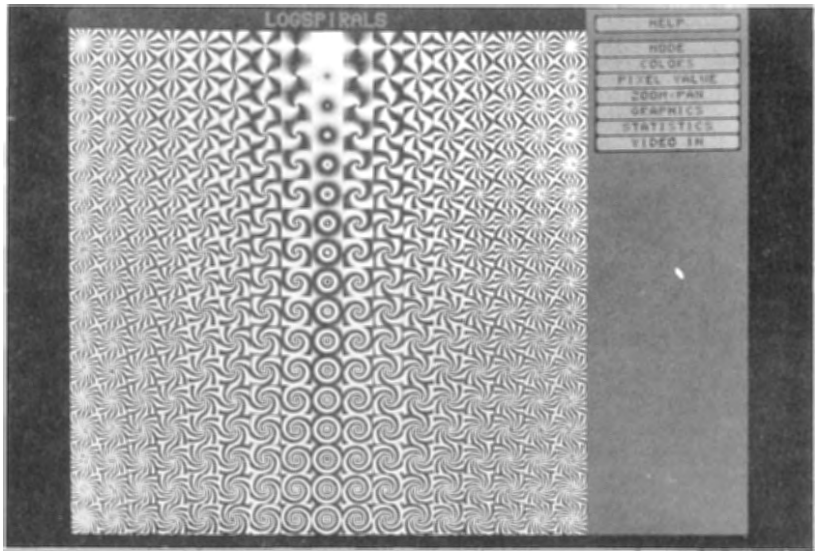

Figure 3: The figure illustrates some neighbourhoods included in the circular symmetry model. The orientation of the model corresponds to the "twistedness" of a neighbourhood and is well-defined.

is obtained. The only singularity is at the origin and does not cause any problem since (21)-(23) are not affected by the values of the integrands at enumerable points (Lebesgue integrals, [12]).

Figure 2 a) illustrates a neighbourhood described by $g(a\xi)$ and Figure 2 b) illustrates $g(b\eta)$. According to the previous sections all neighbourhoods, with iso-gray values being $a\xi + b\eta$ with any real constants a and b, are included in the symmetry model associated with the coordinates $\xi = \ln r$ and $\eta = \varphi$. We will call this type of neighbourhood *circularly symmetric* . Some of the neighbourhoods in this model are given in Figure 3. Figures 4 and 5 illustrate the result of the convolution proposed by (25) with the filter coeficients v^j which are obtained by (26),

$$v^j = \int_0^\infty \int_0^{2\pi} \mu_j(\bar{r}) \exp(-i2\varphi) r dr d\varphi. \tag{31}$$

A plot of these complex valued coefficients is given in [4]. The intensity of the picture in Figure 4 is the certainty in the symmetry, while Figure 5 indicates its orientation at sellected points in the ξ, η domain. By using colour TV monitors it is possible and by far, more convinient to render complex variables. For publishing technical reasons we chose to present the results by means of two images.

The certainty at the borders of the test blocks is approximately half the amount of the block centers, Figure 4. A vertical line in Figure 5 represents circles, while a horizontal line represents star-shaped neighbourhoods. These two neighbourhoods are represented by two different complex variables: the first one has the argument zero, the latter the argument π. The fan-shaped neighbourhoods are mapped to z_1 with $\text{im } z_1 > 0$ or $\text{im } z_1 < 0$ in accordance with the direction of rotation. The amount of "twistedness" that is double the inclination angle of $a\xi + b\eta$, is continuously mapped to the argument of z_1, which can be represented hue in a TV monitor. The dark areas do have an orientation estimate but since the certainty level is too low in these areas, the visibility is automatically suppressed due to the low intensities. An experiment with natural images has been made. The circular symmetry detection is utilized in the classification tasks. Figure 6 illustrates a sea bottom image with sea anemones

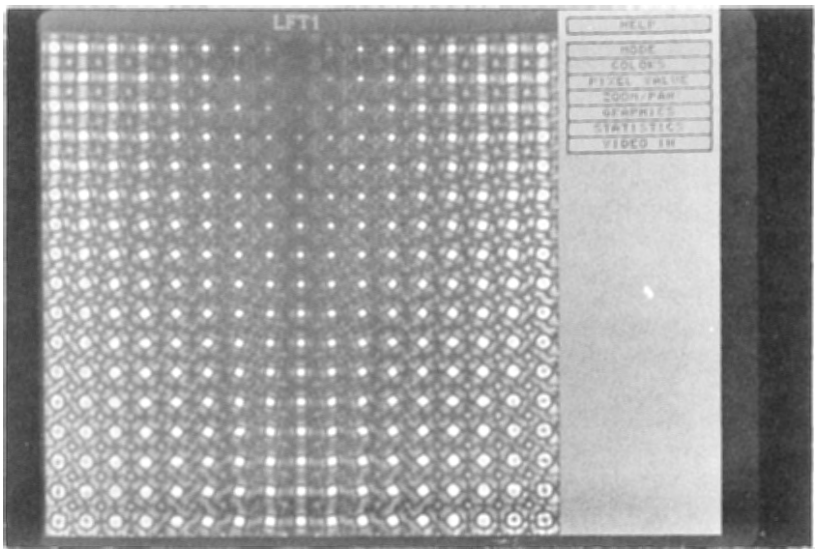

Figure 4: Result of circular symmetry operation on the circularly symmetric neighbourhoods. The intensity represents the certainty.

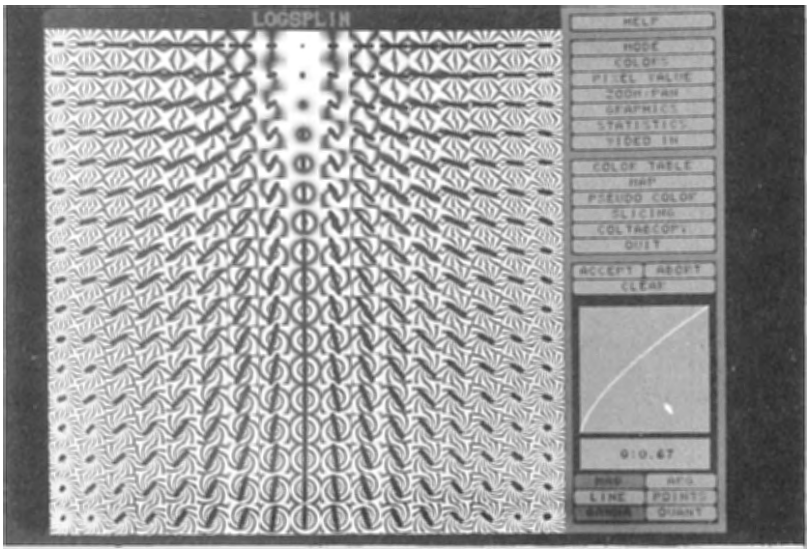

Figure 5: The figure illustrates orientations of the lines in ξ, η domain corresponding to the circular symmetry at selected parts of the original image. The lengths of the bars are proportional to the obtained certainties.

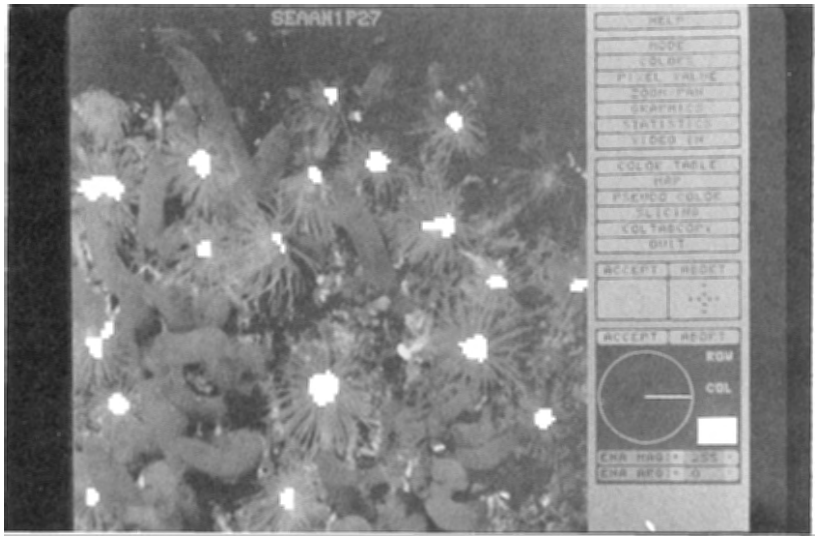

Figure 6: The image is a sea bottom photograph. The objective is to identify the sea anemones. The labels are obtained as a result of box classification.

and their identification only by the circular symmetry image and the original image. Box classification is used.

2. Another pair of harmonic functions, the simplest one, is obtained by the analytic function z:

$$z = x + iy = \xi + i\eta \tag{32}$$

This is simply a model of neighbourhoods having edge or line forms. It delivers the orientation of these lines together with a certainty, [1]. The iso-gray value curves generating these symmetries, *(linear symmetries),* are given in Figure 2 c) and d), that is $g(a\xi)$ and $g(b\eta)$. The necessary filter turns out to be real and a gaussian, [1].

3. Choose the analytic function z^2 to generate the harmonic pair

$$z^2 = x^2 - y^2 + i2xy = \xi + i\eta \tag{33}$$

generating a symmetry which is given in Figure 7 a)-b). We will call this type of symmetry *hyperbolic symmetry.*The corresponding filter coefficients are given by:

$$v^j = \int_0^\infty \int_0^{2\pi} \mu_j(\bar{r}) \exp(i2\varphi) r\, dr\, d\varphi. \tag{34}$$

which is the complex conjugate of the filter obtained for circular symmetry, (31). A number of the neighbourhoods which are included in this model are given in Figure 8. The function generating these is $g(a\xi + b\eta)$ where $\xi = x^2 - y^2$ and $\eta = 2xy$. The neighbourhoods are generated by changing a and b as before. The orientation obtained in this symmetry obviously corresponds to the angle of rotation of the asymptotes. The two asymptotes are orthogonal and make this operator useful for detection of crosses in the natural images. The result of the symmetry detection is given in Figures 9, 10 and 11. The line orientations in Figure 10 uniquely correspond to orientations of the assymptotes of hyperbolas. Figure 11 illustrates the found assymptotes.

4. Yet another symmetry will be generated by the real and the imaginary part of the analytic function $\sqrt{z}$, (the principal branch of the log is utilized):

$$\sqrt{z} = \sqrt{r} \exp(i\frac{\varphi}{2}) = \sqrt{r} \cos(\frac{\varphi}{2}) + i\sqrt{r} \sin(\frac{\varphi}{2}) = \xi + i\eta. \tag{35}$$

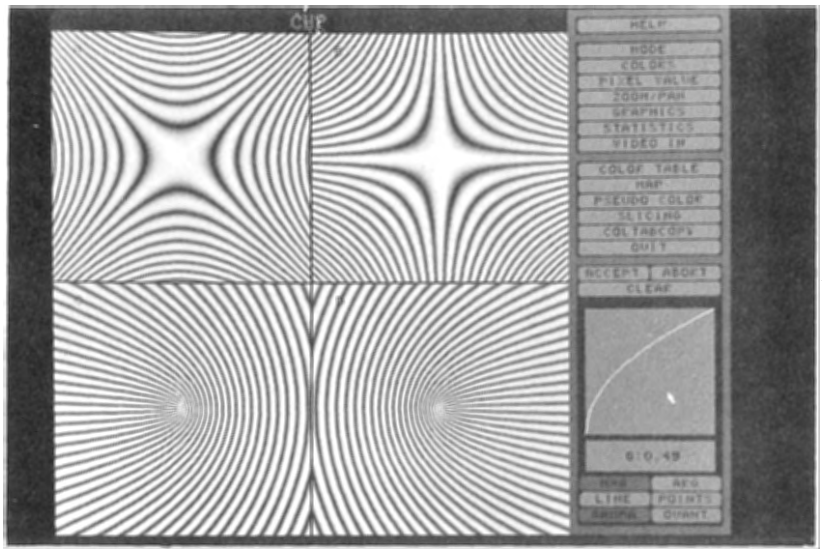

Figure 7: The figure illustrates the iso-gray value curves of a)-b) the hyperbolic symmetric harmonic function pair c)-d) parabolic symmetric harmonic function pair.

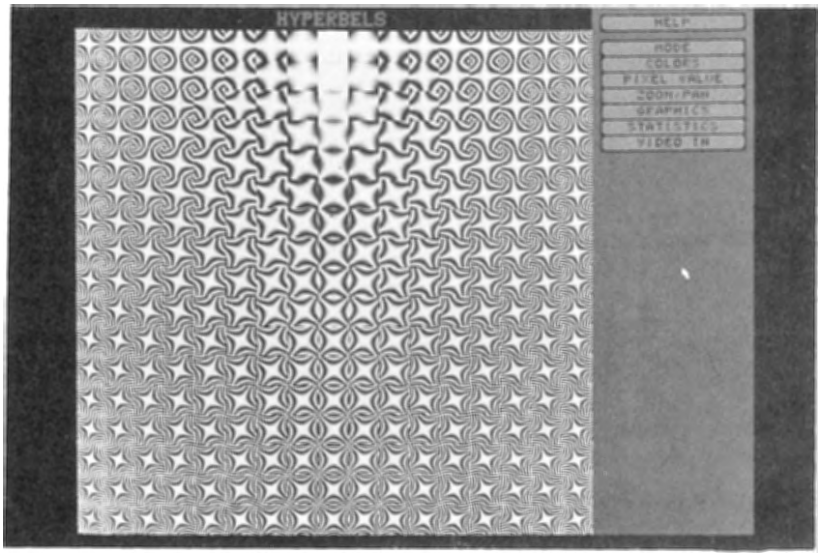

Figure 8: The figure illustrates some neighbourhoods included in the hyperbolic symmetry model. The orientation of the model corresponds to the orientation of the orthogonal asymptotes and is well-defined.

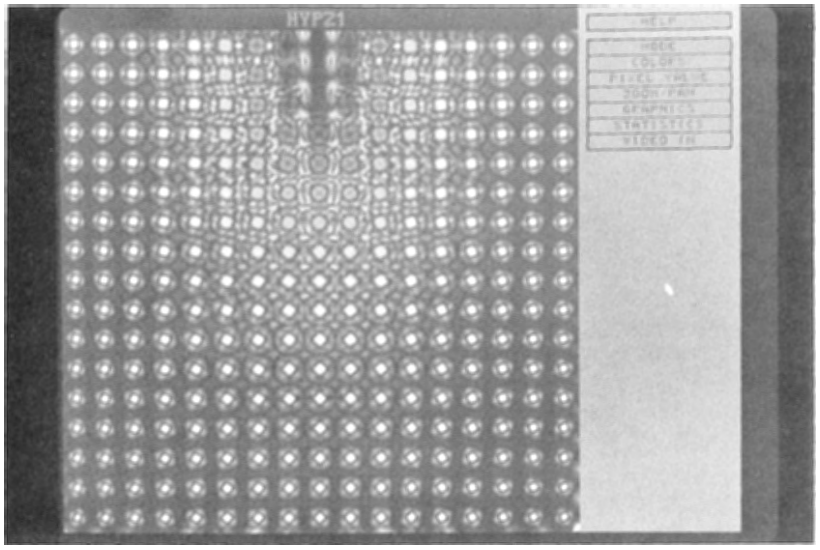

Figure 9: Result of hyperbolic symmetry operation on the hyperbolically symmetric neighbourhoods. The intensity represents the certainty.

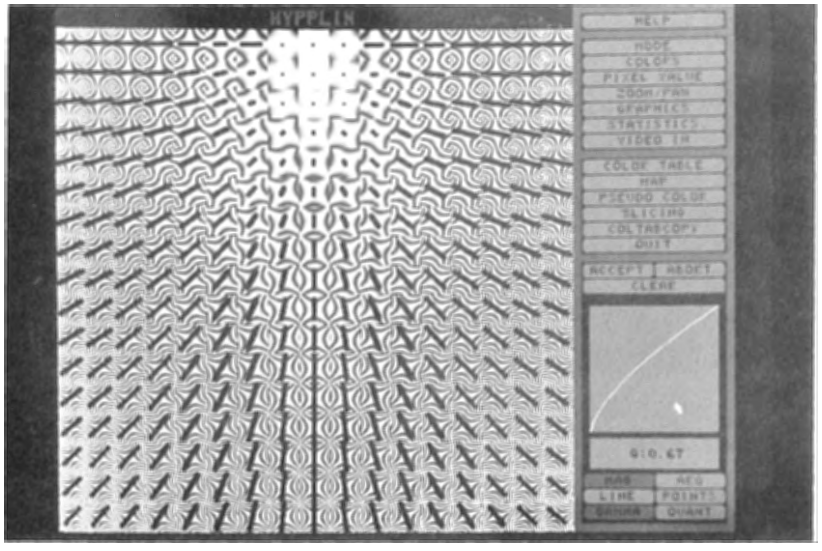

Figure 10: The figure illustrates orientations of the lines in ξ, η domain corresponding to the hyperbolic symmetry at selected parts of the original image. The lengths of the bars are proportional to the obtained certainties.

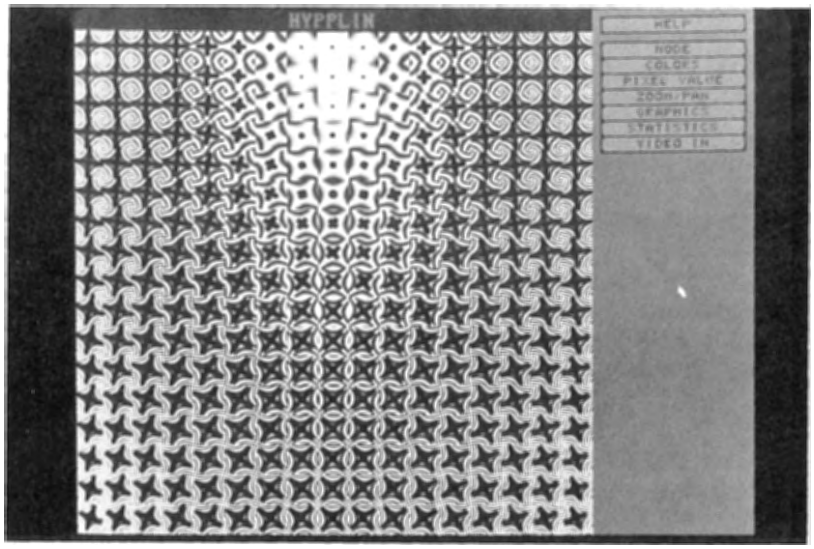

Figure 11: The figure illustrates the assymptotes of hyperbolas corresponding to the orientations of hyperbolic symmetry. The sizes of the crosses are proportional to the obtained certainties.

The symmetric neighbourhood pair generating this symmetry model is given in Figure 7 a)-b). The corresponding filter coefficients are given by:

$$v^j = \int_0^\infty \int_0^{2\pi} \mu_j(\bar{r}) \exp(-i\varphi) r dr d\varphi. \tag{36}$$

This operator is observed to be useful in finger print images to detect patterns having *parabolic symmetries.*The linear combinations of these coordinates, $a\xi + b\eta$, result in rotated versions of the parabolas shown in Figure 7 a)-b).

The list of symmetric patterns detectable by the formula (25) can be made long. It is sufficient to know one of the coordinate curves or its gradient, to be able to construct a symmetry model for the family of curves associated with this curve. In fact, since the the coordinates are assumed to be harmonic and one is the conjugate of the other makes it possible to use the theory developed for harmonic and analytic functions. For example if a coordinate curve function $\xi = u(x, y)$ is known on a circle with radius R and is harmonic within the circle then the other points on the disc are possible to obtain by *Poisson's formula,* [7]:

$$u(z_0) = \frac{1}{2\pi} \int_{|z|=R} \frac{R^2 - |z_0|^2}{|z - z_0|^2} u(z) d\varphi. \tag{37}$$

We have already used the fact that the real and imaginary parts of an analytic function are harmonic and the imaginary part is the harmonic conjugate of the real part.

The results of experiments with energy independent certainty, C_{f2}, are deliberately left out since these are very similar to the results in [1], [4]. However we can comment on the implementation of equation (15)should be made. A threshold value should be specified for the entire image, telling the level below which numerator is considered zero. For values below this threshold the obtained certainties are set to zero. This effectively eliminates the division by zero problem as well since the denominator is greater than the numerator.

5 CONCLUSION

A method to model symmetries of the neighbourhoods in gray value images is derived. It is based on the form of the iso-gray value curves. It is shown that it is possible to check in a special Fourier domain whether all iso-curves in a neighbourhood can be described by an a priori chosen harmonic function pair. However, it is also shown that the equivalent procedure can be performed in the spatial domain without performing a local Fourier transform, which is computationally demanding. For every neighbourhood a complex number is obtained through a convolution of a complex valued image with a complex valued filter. The magnitude of the complex number is the degree of symmetry with respect to the a priori chosen harmonic function pair. The degree of symmetry has a clear definition which is based on the error in the Fourier domain. The argument of the complex number is the angle representing the relative dominance of one of the harmonic pair functions compared to the other.

Since the a priori chosen harmonic function pair is such that the curves associated with these, intersect in right angles (except for some singularities), it is possible to represent a neighbourhood in this curvilinear coordinate system. And hence the problem becomes an edge detection problem in another coordinate system. The obtained orientation corresponds then to the orientation of an edge and therefore has a geometric interpretation. An advantage of using harmonic functions in symmetry descriptions, beside their ability to lead to easily implementable methods, is that one can use many powerful results obtained for analytic functions. The fact that the sum of the maximum and minimum errors for a given neighbourhood is invariant under different tests of symmetry models has potential advantages which can be used to prefer one symmetry model to another in updating the description of the neighbourhoods.

ACKNOWLEDGEMENTS

I should like to thank the Computer Vision Laboratory staff at Linköping University, especially Prof. G. H. Granlund and Dr. H. Knutsson for inspiring discussions. Also the Swedish National Board for Technical Development is acknowledged gratefully for their financial support during the course of this project.

REFERENCES

[1] J. Bigün, G.H. Granlund "Optimal orientation detection of linear symmetry", First International Conf. on Computer Vision, London, June 1987. pp. 433-438

[2] J. Bigün, "Circular symmetry models in image processing", Linköping Studies in Science and Technology thesis No:85, 1986.

[3] J. Bigün, G.H. Granlund "Central symmetry modeling", Third European Signal Processing Conference, The Hague, sep 3-5 1986 pp. 883-886

[4] J. Bigün "Optimal orientatation detection of circular symmetry parameters" submitted for publication. Internal Report LiTH-ISY october 1987.

[5] R. O. Duda, P. E. Hart " Use of the Hough transformation to detect lines and curves in pictures" Comm. ACM 15, 1, January 1972, 11-15.

[6] B. H. Ballard "Generalizing the Hough transform to detect arbitrary shapes" Pattern Recognition 13,2, 1981, 111-112.

[7] L. V. Ahlfors, "Complex Analysis" McGraw-Hill, New york, 1966.

[8] G.H. Granlund: "In Search of a General Picture Processing Operator", Computer Graphics and Image Processing 8, 155–173 (1978).

[9] W.C. Hoffman "The lie algebra of visual perception" J.math. Psychol. 1966 3 p65-98

[10] W.C. Hoffman "Higher visual perception as prolangation of the basic Lie transformation group" Mathematical Biosciences No 6 (1970), pp. 437–471

[11] P. C. Dodwell "The transformation group model of visual perception" Perception & Psychophysics 34 (1) 1983, pp. 1–16

[12] R. L. Wheeden, A Zygmund, "Measure And Integral" Marcel Dekker, Inc., Basel, 1977.